tvst

DOI: 10.1167/tvst.5.5.3

Article

Enhancement of Corneal Visibility in Optical Coherence Tomography Images with Corneal Opacification

Cheuk Wang Chung[1], Marcus Ang[2,3], Mohamed Farook[3], Nicholas G. Strouthidis[2,4,5], Joddhbir S. Mehta[2,3,6], Jean Martial Mari[7], and Michaël J. A. Girard[1,2]

[1] Ophthalmic Engineering and Innovation Laboratory, Department of Biomedical Engineering, Faculty of Engineering, National University of Singapore, Singapore
[2] Singapore Eye Research Institute, Singapore
[3] Singapore National Eye Centre, Singapore
[4] NIHR Biomedical Research Centre, Moorfields Eye Hospital NHS Foundation Trust & UCL Institute of Ophthalmology, London, UK
[5] Discipline of Clinical Ophthalmology and Eye Health, University of Sydney, Sydney, NSW, Australia
[6] Department of Clincal Sciences, Duke-NUS Graduate Medical School, Singapore
[7] Université de la Polynésie française, Tahiti, French Polynesia

Correspondence: Michäel J.A. Girard, Ophthalmic Engineering and Innovation Laboratory, Department of Biomedical Engineering, National University of Singapore, 4 Engineering Drive 3, E4 #04-08, 117583, Singapore. e-mail: mgirard@nus.edu.sg

Received: 13 December 2015
Accepted: 10 July 2016
Published: 8 September 2016

Keywords: anterior segment optical coherence tomography; corneal scar; corneal adaptive compensation; image analysis

Citation: Chung CW, Ang M, Farook M, Strouthidis NG, Mehta JS, Mari JM, Girard MJA. Enhancement of corneal visibility in optical coherence tomography images with corneal opacification. Trans Vis Sci Tech. 2016;5(5):3, doi:10.1167/tvst.5.5.3

Purpose: To establish and to rank the performance of a corneal adaptive compensation (CAC) algorithm in enhancing corneal images with scars acquired from three commercially available anterior segment optical coherence tomography (ASOCT) devices.

Methods: Horizontal B-scans of the cornea were acquired from 10 patients using three ASOCT devices (Spectralis, RTVue, and Cirrus). We compared ASOCT image quality (with and without CAC) by computing the intralayer contrast (a measure of shadow removal), the interlayer contrast (a measure of tissue boundary visibility), and the tissue/background contrast (a measure of overall corneal visibility). All six groups (Spectralis, RTVue, Cirrus, Spectralis+CAC, RTVue+CAC, and Cirrus+CAC) were ranked according to a global performance index that averaged all contrast quantities.

Results: CAC provided mean intralayer contrasts improvement for all devices (all $P < 0.05$). Mean tissue/boundary contrasts were also improved for Spectralis and Cirrus (both $P < 0.001$). Mean interlayer contrasts were increased for Spectralis ($P = 0.011$) only. When comparing global performance indices, all CAC groups outperformed their corresponding baseline groups significantly. RTVue performed best without CAC, but Spectralis+CAC was ranked first.

Conclusions: ASOCT images of corneal scars may be enhanced by CAC through shadow removal, improved tissue boundary visibility, and enhanced corneal visibility against the image background. RTVue produces the finest baseline images but the best image quality can be achieved by applying CAC to Spectralis images.

Translational Relevance: CAC could enhance visibility of corneal images with scars acquired from commercially available ASOCT devices and could aid preoperative planning of patients for ophthalmic procedures.

Introduction

Corneal scars that cause opacity and visual impairment can arise from a wide variety of causes, such as infection, inflammation, trauma, and intraocular surgeries.[1,2] Specifically, infectious diseases such as keratitis and trachoma can generate inflammatory responses that lead to corneal vascularization, and result in corneal opacification.[1,3] Surface abrasion of the cornea can cause temporary scarring as part of the wound healing process, while burns and infections can leave permanent corneal scarring depending on the depth and severity of the initial injury.[4,5] The post-operative cornea can become hazy and opaque while recovering from a normal wound healing response.[6,7] Once corneal scarring becomes permanent and affecting the visual axis, the patient may need to undergo a corneal transplantation.[8] Recent developments in surgical techniques have

enabled surgeons to perform selective replacement of the diseased layer of the cornea – which has led to improved corneal transplant survival and surgical outcomes.[8] Thus, the demand for high-resolution imaging to outline the corneal scar in detail has increased in recent years.

Anterior segment optical coherent tomography (ASOCT) – a noncontact and noninvasive optical imaging technique – is used for the diagnosis and assessment of corneal scars.[9,10] ASOCT has several advantages over other cross-sectional imaging techniques.[11,12] Compared with confocal microscopy, ASOCT has a larger field of view and a faster acquisition speed.[13,14] Unlike ultrasound biomicroscopy, ASOCT does not require the placement of a gel on the cornea for effective imaging.[15,16] ASOCT also provides higher spatial resolution than that of ultrasound biomicroscopy.[15,16] Nevertheless, ASOCT imaging has several limitations. For instance, intense backscattering is observed at the apical area.[13,17,18] Light attenuation causes reduced visibility of the posterior stroma and endothelium.[13,19] In the presence of corneal scarring, the high-opacity regions can generate strong reflections and mask the posterior layers of the cornea.[17,20,21] Clinically, such image defects may pose difficulty in discerning the specific layers of corneal tissue, measuring corneal thickness and estimating the volume and depth of the corneal scar.

We have recently proposed a corneal adaptive compensation (CAC) technique that can be used to improve the quality of ASOCT images from healthy and scarred corneas.[22] Specifically, CAC has been shown to enhance the visibility of the stroma while ensuring low noise over-amplification, thus making endothelium and corneal thickness easily identifiable. Such an algorithm would be beneficial for enhancing clinical interpretation and reducing morphometric errors.[17,19] However, CAC has not yet been quantitatively assessed for all corneal layers. Furthermore, its application has been limited to a small cohort and to a single ASOCT device.

The aim of this study was to establish and to rank the performance of CAC in enhancing corneal images from patients with corneal scars acquired from three commercially available ASOCT devices with resolution of approximately 5 to 7 μm. Our work provides important information to clinicians for using ASOCT (with and without CAC) in the preoperative planning of patients for corneal lamellar procedures.

Methods

Patient Recruitment

We conducted a cross-sectional study of subjects with corneal stromal scars secondary to previous microbial keratitis at the Singapore National Eye Center from January to June 2014. Patients were included if they had significant corneal scarring that required ASOCT imaging for evaluation of the depth and size of the lesion, with no evidence of active infection or inflammation at the time of scanning. Our study was conducted under the approval of the Ethics Committee of the SingHealth Centralized Institutional Review Board (CIRB) with informed consent, in accordance with the tenets of the Declaration of Helsinki.

ASOCT Imaging

Each eye had three horizontal ASOCT scan volumes performed by a trained operator (FM) using three different commercially available spectral-domain (SD) ASOCT systems: (1) Spectralis (Heidelberg Engineering, Vista, CA) combines a scanning laser ophthalmoscope (SLO) with optical coherence tomography (OCT) to produce tracking laser tomography that has a 7-μm axial resolution and scans at 40,000 A-scans per second, (2) RTVue (Optovue Inc, Fremont, CA), which uses an 830-nm laser wavelength, 2.3-mm imaging depth, and provides 26,000 A-scans per second, 15-μm transverse resolution, and 5-μm axial resolution in tissue, and (3) Cirrus (Carl Zeiss Meditec, Dublin, OH) is an SD OCT platform that has a 5-μm axial resolution and scans at 27,000 A-scans per second.

Compensation Techniques for the Cornea

To enhance ASOCT images of the cornea, we previously applied standard compensation (SC) and adaptive compensation (AC) techniques to amplify the weakened signals (due to light attenuation) in the deep part of the cornea.[23,24] Both techniques can improve the visibility of optic nerve head tissues, and that of coronary arteries in OCT images.[25–27] However, for the cornea, SC consistently over-amplified noise below the endothelial layer; AC was able to reduce noise over-amplification in the central region, but was less effective in the peripheral regions.[22] This is due to the prolate geometry of the cornea, whereby corneal tissues can appear in

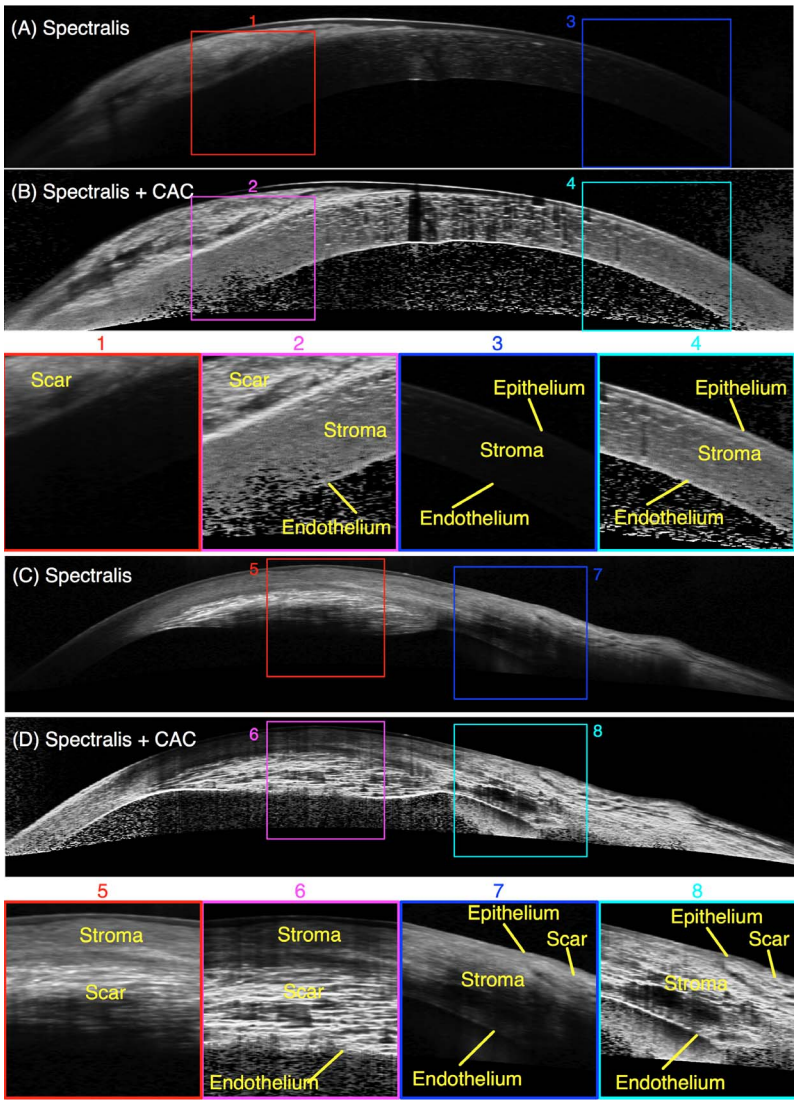

Figure 1. Corneal images acquired by Spectralis ASOCT device, processed (B, D) with or (A, C) without CAC. Stroma and endothelium posterior of scarred tissue were detectable after applying CAC (*Squares 1, 2*). At the peripheral cornea, visibility of epithelium, stroma, and endothelium was improved after applying CAC (*Squares 3, 4*). Posterior corneal scar and endothelium were more visible after applying the CAC technique (*Squares 5, 6*). Posterior stroma and endothelium were detectable after using CAC (*Squares 7, 8*).

both anterior and posterior regions of an ASOCT image.

Corneal Adaptive Compensation

We developed CAC to address the drawbacks exhibited by SC and AC.[22] Briefly, CAC amplifies the attenuated light intensity as it travels through the depth of cornea. The amplification factor increases exponentially with the tissue (image) depth to compensate for the corresponding exponential weakening in light intensity. To prevent noise over-amplification near the endothelial layer, a compensation limit is set, beyond which the amplification factor remains constant. The compensation limit is automatically set at a different depth for each A-scan to adapt to the prolate geometry of the cornea.

CAC has been shown to enhance the visibility of the stroma with low noise over-amplification in the background, making the thickness of the endothelium and that of the cornea easily identifiable (see image examples from three ASOCT devices with and without CAC in Figs. 1–3).[22]

For this study, all ASOCT images (Spectralis, RTVue, and Cirrus) with corneal opacification were post-processed with CAC (Spectralis+CAC, RTVue+CAC, and Cirrus+CAC). As the extent of

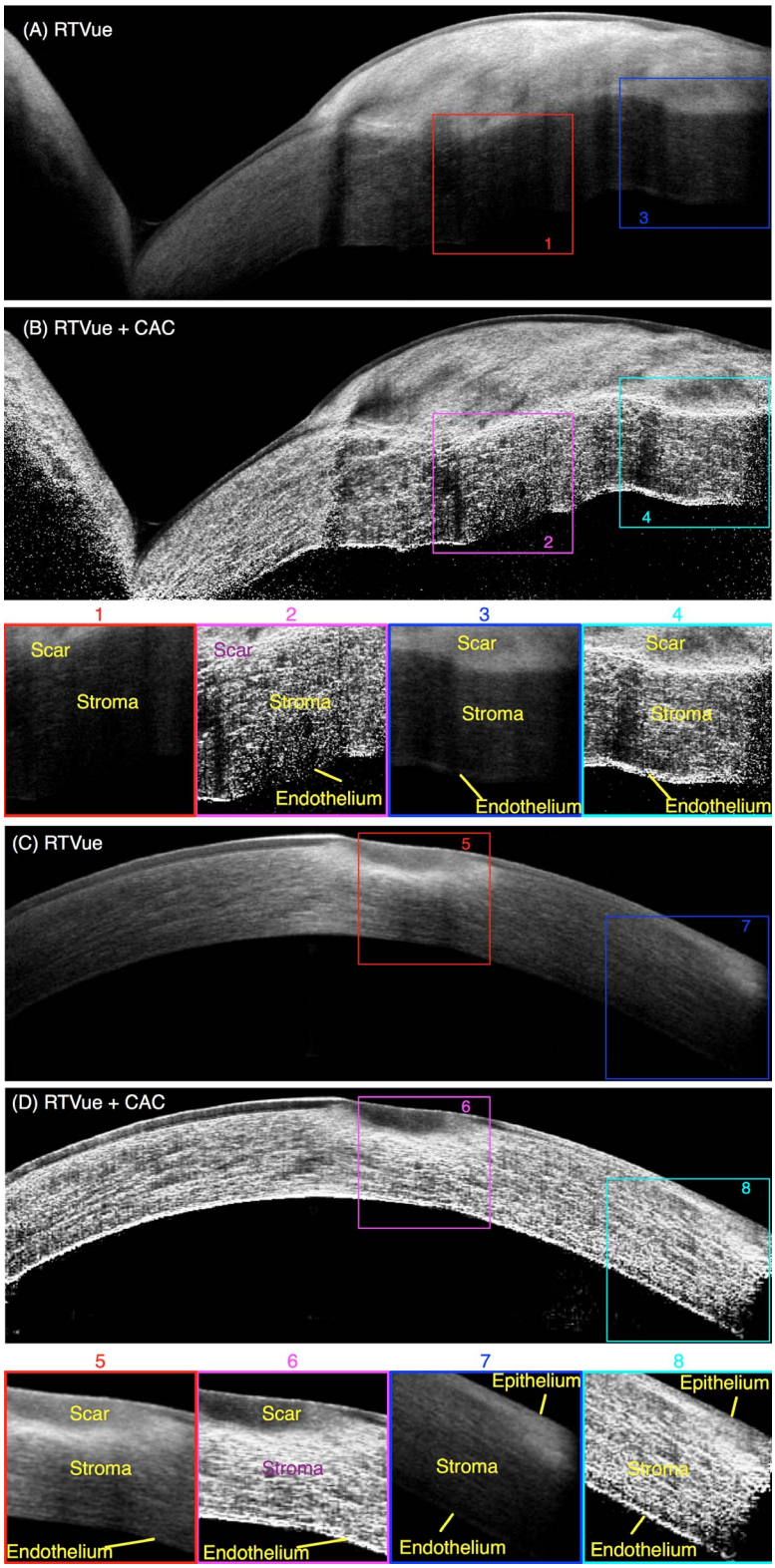

Figure 2. Corneal images acquired by RTVue ASOCT device, processed (B, D) with or (A, C) without CAC. Stroma and endothelium posterior of scarred tissue were detectable after applying CAC (*Squares 1, 2*). The light intensity of stroma became more uniform after applying CAC (*Squares 3, 4*). The visual contrast between scar and stroma was improved in post-CAC image (*Squares 5, 6*). The visibility of peripheral corneal tissue was improved after using CAC (*Squares 7, 8*).

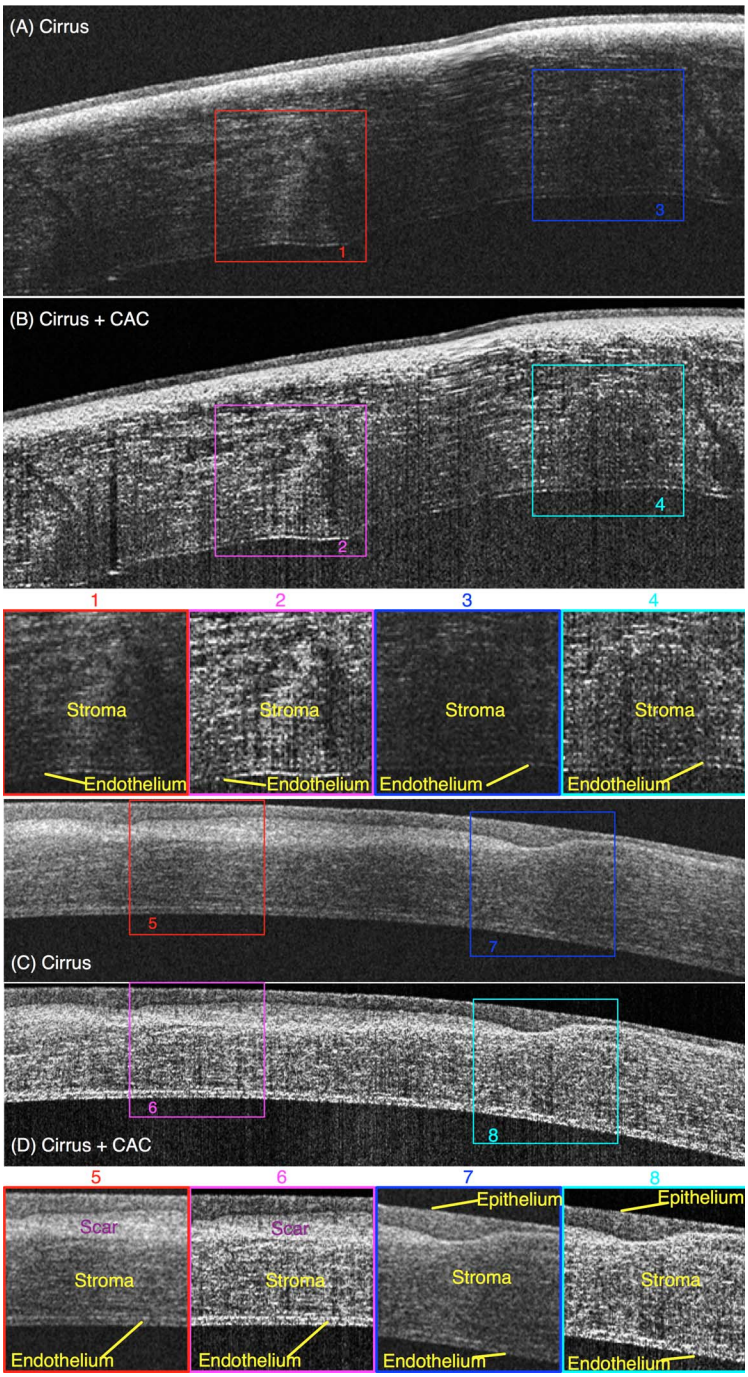

Figure 3. Corneal images acquired by Cirrus ASOCT device, processed (B, D) with or (A, C) without CAC. The intensity of stroma and endothelium was more uniform in the CAC image than that in the baseline one (*Squares 1, 2*). Shadow was removed from the stroma after applying the CAC technique (*Squares 3, 4*). The visibility of stroma and endothelium was improved in post-CAC image (*Squares 5, 6*). The visibility of epithelium and endothelium improved after using the CAC technique (*Squares 7, 8*).

light attenuation is device-specific, threshold exponents were chosen independently for each ASOCT device and they varied from 8.0 to 12.0 for Spectralis, 8.0 to 30.0 for RTVue, and 2.0 to 14.0 for Cirrus. Note that the threshold exponent indicates the depth at which compensation is stopped to limit the effects of noise over-amplification. A compensation contrast exponent of 2 was also selected for all images and all devices.

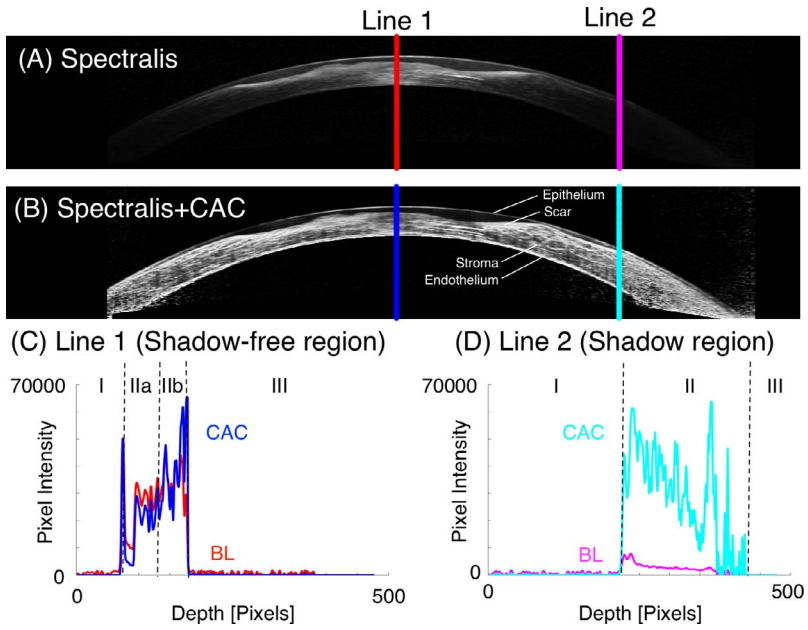

Figure 4. Corneal images are from Spectralis ASOCT device (A) before and (B) after applying the CAC algorithm. *Lines 1 and 2* indicate the directions of A-scans crossing the shadow-free and shadow regions in both images, respectively. Plots (C) and (D) show A-scan pixel intensity against depth corresponding to *Lines 1 and 2*. Area II indicates the region within the cornea while *Areas IIa and IIb* are the anterior and posterior corneal regions, respectively. *Areas I and III* are the image background.

Intralayer Contrast

The intralayer contrast can be used to assess the performance of CAC as it measures whether shadow artefacts (from scars) are visible within a given corneal layer. To verify that CAC can eliminate shadowing, we computed the intralayer contrast for each layer before and after applying CAC.

To calculate the intralayer contrast, we chose two regions of interest (ROI) within shadow-free and shadowed regions (ROI_1 and ROI_2) of a given corneal layer (Fig. 5, Squares 1, 2). Each ROI was 5×5 pixels to accommodate thin corneal layers (e.g., endothelium), and regions within the scar. The intralayer contrast was defined as $1 - |(I_1 - I_2) / (I_1 + I_2)|$,[23] where I_1 and I_2 were the mean pixel intensities of ROI_1 and ROI_2, respectively. The intralayer contrast varied between 0 and 1, with values close to 1 indicating the absence of scar shadowing, and values closer to 0 indicating shadowing.

Interlayer Contrast

The interlayer contrast was a measure of boundary visibility across two corneal layers. To verify that CAC can improve the visibility of tissue boundaries, we evaluated the interlayer contrasts across multiple tissue boundaries (i.e., epithelium/stroma, epithelium/scar, stroma/scar, endothelium/stroma, and endothelium/scar), before and after CAC.

To calculate the interlayer contrast, we chose two ROIs (ROI_3 and ROI_4; 5×5 pixels) in two shadow-free adjacent corneal layers (Fig. 6, Squares 1, 2). The interlayer contrast was defined as $|(I_3 - I_4) / (I_3 + I_4)|$,[23] where I_3 and I_4 were the mean pixel intensities of ROI_3 and ROI_4, respectively. The interlayer contrast varied between 0 and 1. A value close to 0 indicated the boundary between adjacent tissues was poorly detectable, whereas that close to 1 indicated a highly detectable boundary.

Tissue/Background Contrast

The tissue/background contrast measured the visibility of the anterior and posterior corneal boundaries against the ASOCT image background. The tissue/background contrast was calculated similarly to the interlayer contrast but for the endothelium/background and epithelium/background boundaries. Here, ROI_3 was located either in the epithelium or the endothelium (shadow-free), while ROI_4 in the background anterior or posterior to the cornea (Fig. 6, Diamonds 5, 6). As for the interlayer contrast, the tissue/background contrast varied between 0 and 1. A value near 0 indicated that the anterior or posterior corneal boundary was poorly detectable, whereas that close to 1 indicated a highly detectable boundary.

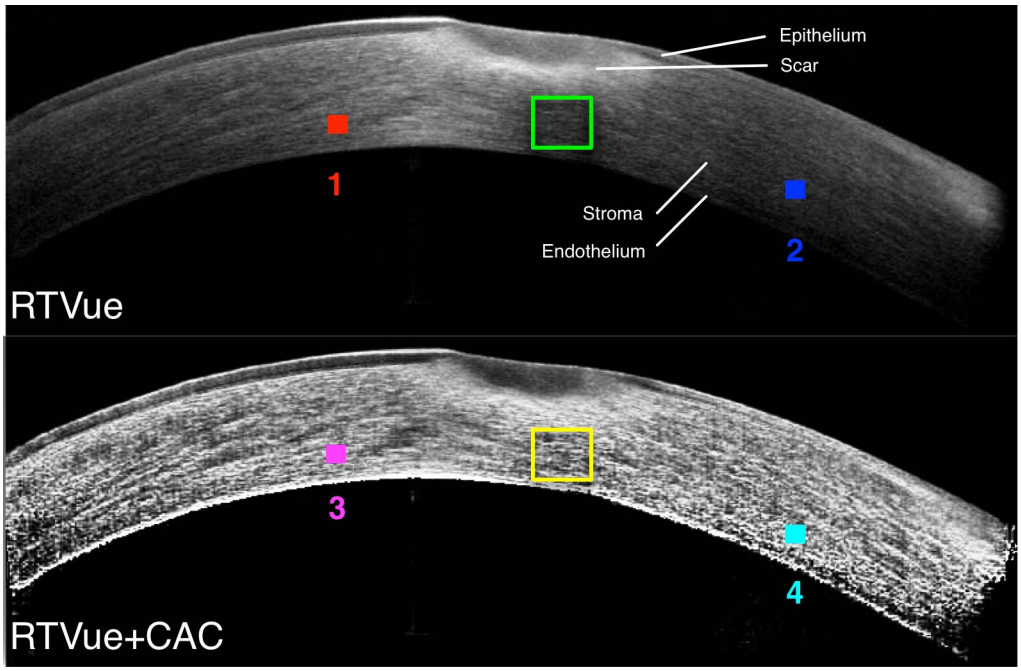

Figure 5. ROIs are located in the shadow-free (*Squares 1, 3*) and shadow (*Squares 2, 4*) regions of stroma for calculating intralayer contrast in RTVue (without CAC) and RTVue+CAC images. The average intensity value within each ROI is used to calculate the individual intralayer contrast. The intralayer contrasts are similarly calculated for the endothelium and the scar. Scar shadow is cast on the stroma (*green square*) and the shadow is removed after applying CAC (*yellow square*). The *squares* represent the ROIs are enlarged for illustration purposes.

Statistical Analysis

To ascertain that image enhancement imposed by CAC was significant, we conducted unpaired one-tailed *t*-tests on the intralayer, interlayer, and tissue/background contrasts computed from the baseline (BL) and CAC images produced by each device. A result was considered significant if the *P* value was less than 0.05. All statistical analyses were performed using MATLAB (version 2012b; The MathWorks, Inc., Natick, MA).

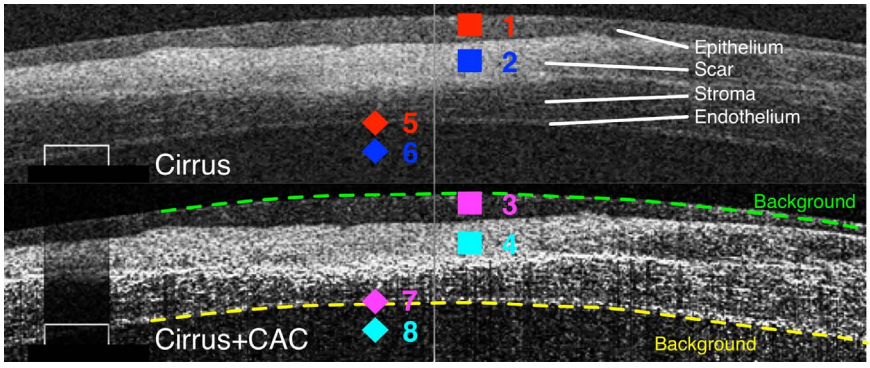

Figure 6. ROIs are located in the epithelium (*Squares 1, 3*) and scar (*Squares 2, 4*) for calculating interlayer contrast in Cirrus (without CAC) and Cirrus+CAC images. The average intensity value within each ROI is used to calculate the epithelium/scar interlayer contrast. Similarly, the interlayer contrasts are calculated for the epithelium/stroma, endothelium/stroma, endothelium/scar, and stroma/scar. The regions above the epithelium (*green line*) and below the endothelium (*yellow line*) are the image background. Another set of ROIs is located in the endothelium (*Diamonds 5, 7*) and background (*Diamonds 6, 8*) for calculating endothelium/background contrast in Cirrus (without CAC) and Cirrus+CAC images. The epithelium/background contrast is also calculated in similar manner. The *squares* and *diamonds* are enlarged for illustration purposes.

Table 1. Comparison (*P* Value) of Intralayer Contrasts before and after Applying CAC on ASOCT Images Obtained from Spectralis, RTVue, and Cirrus Devices

	Spectralis ($n = 7$)	Spectralis + CAC ($n = 7$)	*P* Value	RTVue ($n = 12$)	RTVue + CAC ($n = 12$)	*P* Value	Cirrus ($n = 17$)	Cirrus + CAC ($n = 17$)	*P* Value
Endothelium	.70 ± .22	.93 ± .05	**0.016**	.61 ± .13	.82 ± .11	**<0.001**	.82 ± .11	.82 ± .16	0.511
Stroma	.36 ± .10	.79 ± .12	**<0.001**	.59 ± .17	.92 ± .06	**<0.001**	.86 ± .09	.92 ± .06	**0.012**
Scar	.72 ± .17	.86 ± .09	**0.046**	.76 ± .13	.91 ± .08	**0.001**	.79 ± .12	.89 ± .09	**0.003**
Mean intralayer contrast	60 ± .08	.86 ± .06	**<0.001**	.65 ± .08	.88 ± .04	**<0.001**	.82 ± .07	.88 ± .06	**0.013**

Statistical significance ($P < 0.05$) is highlighted in bold.

Assessment of ASOCT Devices with and without CAC

To assess the overall performance of all three ASOCT devices with and without CAC, we defined a global performance index. This latter was calculated for each group (Spectralis, Cirrus, RTVue, Spectralis+CAC, Cirrus+CAC, RTVue+CAC) by averaging the intralayer contrasts (all corneal layers), the interlayer contrasts (all boundaries), and the tissue-boundary contrasts (all boundaries). Statistical analyses (unpaired two-tailed *t*-tests) were performed to ascertain that there was significant difference ($P < 0.05$) in image quality between any two groups.

Results

Comparison of Baseline and CAC ASOCT Images

Baseline ASOCT images acquired from scarred cornea contained several artifacts and exhibited poor tissue boundary contrast. Corneal scars were highly visible while posterior stroma and peripheral region were underexposed (Fig. 1, Squares 1, 3; Fig. 2, Square 7). Opaque scars also cast shadows on some part of the posterior layers, resulting uneven light intensity of the stroma tissue (Fig. 2, Square 3; Fig. 3, Square 1). Moreover, endothelium and scar–stroma boundary were unclear due to poor contrast between adjacent tissues (Fig. 1, Square 5; Fig. 3, Square 3).

CAC was able to enhance the baseline ASOCT images. Previously underexposed tissues were visible together with the scar after applying CAC (Fig. 1, Squares 2, 4; Fig. 2, Square 8). Tissue visibility posterior to the scars was also improved (Fig. 2, Square 4; Fig. 3, Square 2). Endothelium and scar–stroma boundary became detectable (Fig. 1, Square 6; Fig. 3, Square 4). Furthermore, anterior and posterior corneal boundaries were observable as the background signal was not over-amplified (Figs. 1–3). The results show that the CAC technique provides clinicians with an advantage in visualizing corneal scar in ASOCT images.

Verification of Image Improvement in A-Scans

To assess the performance of CAC, we investigated how A-scan signals varied as a function of depth before and after applying CAC (Fig. 4). In the shadow-free region (Line 1), the CAC technique reduced the background noise (Fig. 4C, Areas I, III). Consequently, the cornea became visible from the background with high contrast. CAC also lowered the signal intensity in the anterior cornea (Fig. 4C, Area IIa) while improving that in the posterior region (Fig. 4C, Area IIb). This resulted in improved corneal visibility throughout the corneal thickness. In the shadowed region (Line 2), CAC amplified the tissue signal (Fig. 4D, Area II) to increase tissue visibility without over-amplifying the background noise (Fig. 4D, Areas I, III).

CAC Eliminated Scar Shadows

The visibility of shadowed regions in all images was improved after applying CAC. The mean intralayer contrasts increased significantly in all devices (mean increase: Spectralis 0.26, $P < 0.001$; RTVue 0.23, $P < 0.001$; Cirrus 0.06, $P = 0.013$). CAC removed shadows from all layers (Spectralis and RTVue; Table 1). For Cirrus, shadow removal was significant only for the stroma and scar layers.

Table 2. Comparison (*P* Value) of Interlayer Contrasts before and after Applying CAC on ASOCT Images Obtained from Spectralis, RTVue, and Cirrus Devices

	Spectralis ($n = 7$)	Spectralis + CAC ($n = 7$)	*P* Value	RTVue ($n = 12$)	RTVue + CAC ($n = 12$)	*P* Value	Cirrus ($n = 17$)	Cirrus + CAC ($n = 17$)	*P* Value
Epithelium/stroma	.31 ± .12	.40 ± .20	0.167	.20 ± .15	.26 ± .16	0.165	.25 ± .15	.25 ± .17	0.520
Endothelium/stroma	.19 ± .18	.39 ± .13	**0.018**	.20 ± .16	.34 ± .14	**0.017**	.26 ± .19	.32 ± .17	0.171
Epithelium/scar	.16 ± .06	.39 ± .20	**0.011**	.18 ± .08	.33 ± .09	**<0.001**	.15 ± .09	.32 ± .11	**<0.001**
Endothelium/scar	.48 ± .32	.47 ± .24	0.518	.73 ± .23	.40 ± .23	0.999	.59 ± .11	.49 ± .16	0.980
Stroma/scar	.38 ± .16	.33 ± .13	0.729	.44 ± .25	.37 ± .26	0.732	.25 ± .15	.26 ± .13	0.406
Mean interlayer contrast	.30 ± .05	.40 ± .06	**0.011**	.35 ± .09	.34 ± .07	0.784	.30 ± .05	.33 ± .06	0.142

Statistical significance ($P < 0.05$) is highlighted in bold.

CAC Enhanced the Visibility of Corneal Layer Boundaries

We found that CAC improved the visibility of tissue boundaries for Spectralis as indicated by the 0.10 increase in mean interlayer contrast ($P = 0.011$; Table 2). For Cirrus and RTVue, there were no statistically significant differences in mean inter-layer contrasts between BL and CAC images.

Specifically, for the anterior scar boundary (epithelium/scar), there was a significant increase in interlayer contrast after applying CAC and this was true for all devices ($P < 0.05$). However, for the posterior scar boundary (scar/stroma), there were no significant differences (all devices). This latter result is expected because of the poor tissue visibility below scars in BL images.

After applying CAC, the endothelium/stroma interlayer contrasts increased for all devices (significant for Spectralis and RTVue, $P < 0.05$, but not Cirrus).

CAC Increased the Visibility of Cornea against the Background

The anterior and posterior corneal boundaries became more visible for all devices after applying CAC due to the increase in epithelium/background and endothelium/background contrasts (significant for both boundaries and all devices, $P < 0.05$, except for the endothelium/background contrast with RTVue; Table 3).

Table 3. Comparison (*P* Value) of Tissue/Background Contrasts before and after Applying CAC on ASOCT Images Obtained from Spectralis, RTVue, and Cirrus Devices

	Spectralis ($n = 7$)	Spectralis + CAC ($n = 7$)	*P* Value	RTVue ($n = 12$)	RTVue + CAC ($n = 12$)	*P* Value	Cirrus ($n = 17$)	Cirrus + CAC ($n = 17$)	*P* Value
Epithelium/background	.89 ± .06	.99 ± .00	**0.002**	.92 ± .05	.99 ± .01	**<0.001**	.68 ± .07	.89 ± .05	**<0.001**
Endothelium/background	.85 ± .08	.92 ± .05	**0.028**	.85 ± .18	.92 ± .14	0.148	.20 ± .10	.38 ± .15	**<0.001**
Mean tissue/background contrast	.87 ± .04	.96 ± .03	**<0.001**	.88 ± .11	.95 ± .07	0.080	.44 ± .07	.64 ± .09	**<0.001**

Statistical significance ($P < 0.05$) is highlighted in bold.

Ranking of ASOCT Devices with and without CAC

Without CAC, RTVue outperformed the other two devices when considering mean interlayer contrasts and mean tissue/background contrasts (Figs. 7B, 7C). Although RTVue was ranked behind Cirrus in the mean intralayer contrast (Fig. 7A), RTVue scored higher than Cirrus in the global performance index (mean difference 0.11, $P < 0.001$). However, there was no significant difference in the aggregate image quality between RTVue and Spectralis (Table 4).

Overall, Spectralis+CAC emerged the best in terms of global performance index (Fig. 7D). All CAC groups outperformed their corresponding BL groups significantly. Aggregate image quality from Spectralis+CAC and RTVue+CAC groups were significantly better than others, but there was no significant difference between the two groups (Table 4).

Discussion

In this study, we tested and ranked the performance of CAC in enhancing corneal images from the same scar acquired with three different commercially available ASOCT devices. In order to test the consistency of the results on various densities of scars, we tested out the enhancement on 10 different patients. We reported that CAC improved the image quality in all three ASOCT devices. We also showed that Spectralis+CAC provided the best image quality, which was superior to that of the best device that did not employ CAC (RTVue). Our results may encourage the use of CAC in corneal clinics to aid in the diagnostic planning of lamellar surgery.

CAC Enhanced the Quality of ASOCT Images

In this study, we found that CAC enhanced the quality of ASOCT images in three major ways. First, CAC was able to correct scar shadows (Figs. 4A, 4B, Line 2). Specifically, our results indicated that, after applying CAC, the mean intralayer contrast increased, and this was true for all devices (Table 1). In fact, shadow removal by CAC was evident in all layers for both the Spectralis and the RTVue. The stroma, the endothelium and the posterior scar tissue all became more visible after applying CAC. CAC was able to generate a cross-sectional view of the cornea with its full thickness, which may aid in the full ascertainment of the depth of the lesion to ascertain the most appropriate keratoplasty procedure.[3]

Second, CAC improved the visibility of the corneal layer boundaries. We reported increased mean interlayer contrasts for Spectralis, but not for RTVue and Cirrus, after applying CAC (Table 2). Specifically, the epithelium/scar contrasts were improved in CAC images for all devices but the endothelium/stroma contrasts increased for Spectralis and RTVue only. The endothelium/scar and stroma/scar contrasts were not significantly improved for Spectralis and RTVue. However, note that these baseline contrasts are artificially large due to the low tissue visibility below the scars.[24] Therefore, the baseline interlayer contrasts cannot be representative of endothelium/scar and stroma/scar boundaries visibility. In other words, CAC does not necessarily increase these contrasts because of shadow removal (increased visibility) within the stroma and endothelium underneath the scar. Nevertheless, an enhancement in interlayer contrast, as obtained with CAC for several boundaries, may be clinically relevant for identifying scarred region following infection or inflammation and also for estimating flap depth after laser in situ keratomileusis.[3]

Third, CAC considerably improved the contrast of the cornea against its image background (Fig. 6). Specifically, we found that the mean tissue/background increased for CAC images in Spectralis and Cirrus (Table 3). The epithelium became more visible after applying CAC and this was true for all devices, while the visibility of endothelium improved in Spectralis and Cirrus. In other words, our result suggests that CAC can improve the visibility of the anterior and posterior corneal boundaries without amplifying the background noise. This is of high interest, because CAC may enable an accurate measurement of corneal thickness that is important in planning refractive and corneal surgery[11] it may also be useful in the longitudinal follow-up of patients with corneal edema.[28]

Other than assessing image enhancements produced by CAC, we also developed a global performance index to quantify the overall image quality of ASOCT devices with and without CAC (Table 4), such an index is a succinct representation of a device's performance in eliminating shadows, enhancing corneal layer boundaries, and improving corneal visibility against the image background. We found that applying CAC to the Spectralis images produced the best image quality, but when CAC was not used, the RTVue device outperformed the others (Fig. 7).

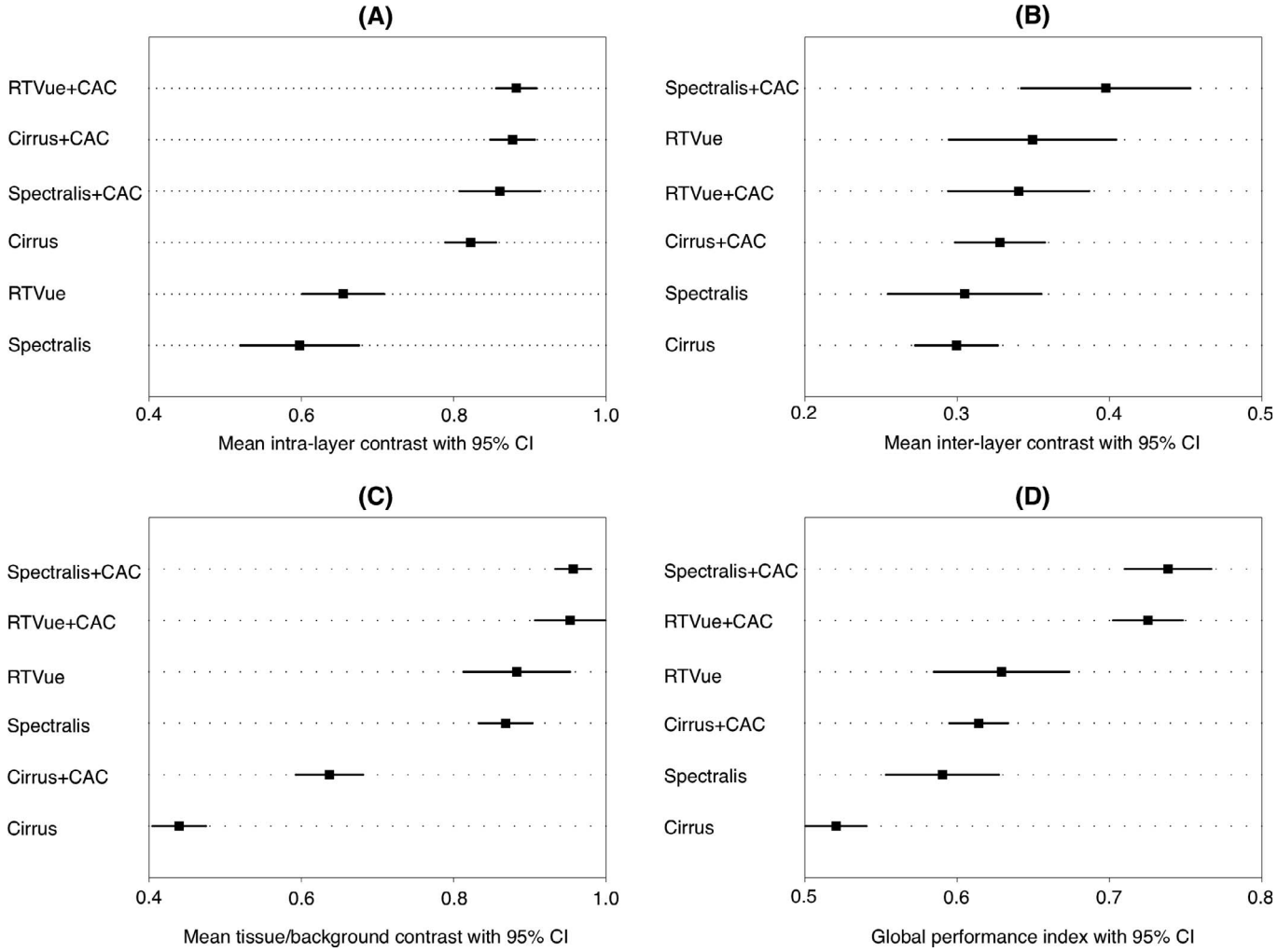

Figure 7. (A) Mean intralayer contrast, (B) mean interlayer contrast, (C) mean tissue/background contrast, and (D) global performance index. The methods are ranked according to the mean contrast or index (*filled squares*) and the best performing method is at the top. Each *bold horizontal line* represents the 95% confidence interval (CI) about the mean value.

Translational Relevance of Current Work

Our work has important clinical implications. First, advances in corneal transplantation techniques permit selective replacement of the stroma or endothelial tissue.[29] The procedures are technically complicated and demand high-resolution images for measuring layer depth and clarifying its composition.[3]

Table 4. Multiple Pair-Wise Comparisons of the Global Performance Index

	Spectralis	Spectralis+CAC	RTVue	RTVue+CAC	Cirrus	Cirrus+CAC
Spectralis						
Spectralis+CAC	**0.15*** **					
RTVue	**0.04**	*−0.11***				
RTVue+CAC	**0.13*** **	*−0.01*	**0.10*** **			
Cirrus	*−0.07*** *	*−0.22*** *	*−0.11*** *	*−0.20*** *		
Cirrus+CAC	**0.02**	*−0.12*** *	*−0.01*	*−0.11*** *	**0.09*** **	

Bolded values indicate that the method in the left column performs better than that in the first row, and italic the inverse. Global performance index comparing two methods. *$P < 0.05$. **$P < 0.01$. ***$P < 0.001$.

ASOCT offers cross-sectional corneal images of high quality and is currently used to assess corneal and anterior segment parameters in healthy subjects.[11,12] By coupling ASOCT images with CAC, the visibility of corneal lesions and scars, may be improved. The enhanced ASOCT images can afford major advantages in examining diseased corneal layers by enhancing en face corneal images,[30] or even improving visualization of corneal vascularization,[31] when evaluating suitable surgical options and monitoring post-surgery outcomes. In the future, CAC could be applied as a software enhancement to several of the developing intraoperative ASOCT machines currently available, as well as aiding corneal incision construction in machines currently used for femtocataract procedures.[32]

Second, experienced photographers and clinicians often reacquire images with different acquisition parameters to show the area or layer of interest. However, repeated image acquisitions are not always feasible as the prolonged imaging process can lengthen patients' waiting time and cause increased discomfort to the patients. The CAC technique can enhance the images and allow clinicians to extract valuable information such as thickness of cornea scar and shape of the cornea, especially in the raw images with poor corneal visibility. CAC can be applied on images captured with optimized acquisition parameters to produce better images.

Limitations of Current Work

Several limitations in this work warrant further discussion. First, we used small and constant-size ROIs for all contrast calculations. While it is feasible to use different ROIs in different images, it was difficult to decide on a specific rule-of-thumb that would determine the size of each ROI. Due to the presence of thin layers (endothelium and epithelium), we were required to use small ROIs (5×5 pixels). For consistency, we used the same ROI size for all other layers. Furthermore, small ROIs are desirable for targeting the shadowed or underexposed regions and suitable for assessing the image enhancements provided by the CAC technique. For verification, we have re-performed contrast measurements using larger ROIs (10×10 and 20×20 pixels) and our results were consistent for the thickest corneal layers (on average, 15.6% difference in contrast values when comparing contrast results from small and large ROIs). None of our conclusions were also affected by a change in ROI size. This suggests that small ROIs are representative even for the thickest corneal layers.

Second, we used a global performance index to rank devices. This index is representative of image quality based on criteria such as shadow removal, improving intertissue boundaries, and enhancing corneal visibility against the image background. Although other image quality measures such as mean squared intensity difference[33] and signal-to-noise ratio[34] are available, they were not developed specifically for ASOCT images. In contrast, our global performance index relates to the visibility of corneal layers and is clinically relevant.

Third, we were unable to compare CAC images with those obtained from tissue histology to ascertain the 'true' tissue boundary locations. The OCT images were obtained from patients in vivo, therefore we could not perform tissue histology (on their corneas) to compare with the CAC images. However, previous studies established that the OCT cross-sections on scarred corneas were comparable to those obtained from light microscopy.[9] Furthermore, when the scar boundaries were visible, their locations were highly similar in both baseline and CAC images (Fig. 1, Squares 5, 6; Fig. 2, Squares 3, 4; Fig. 3, Squares 5, 6). Overall, the results indicate that CAC enhanced the visibility of 'true' scar boundaries in OCT images.

Fourth, it is possible for clinicians to perform several acquisitions with different signal strength, contrast, and averaging window to produce better images. The images can be enhanced further by applying CAC. In several ASOCT images acquired with different signal strengths and contrasts but from the same patient, the interlayer contrasts of the images improved after applying CAC. The results indicated that CAC is capable of producing images to show specific area or layer of interest, with or without hardware adjustment. More importantly, adjusting the signal strength and contrast cannot eliminate image artifacts, such as shadows at peripheral cornea and light attenuation at deeper stroma and endothelium posterior of scar. The averaging technique also unlikely to correct the artifacts as it is often used to eliminate speckle noise in OCT images.[35] Nevertheless, the visibility of shadowed regions can be improved by applying the CAC technique (Figs. 1–3). Overall, the images enhanced by CAC are better than those modified by adjusting the acquisition parameters.

As a final caveat, we do not claim that all aspects of ASOCT image quality are improved with CAC. Specifically, CAC enhances ASOCT images by

amplifying attenuated signals in shadowed regions, by increasing contrast between different tissues, and by promoting corneal visibility against the image background. Other image quality factors such as image resolution, tissue penetration depth, and noise levels are device-specific and out of our control in a post-processing analysis. Another limitation is that while enhancement of the normal corneal tissue and anatomic boundaries surrounding the pathology are enhanced by the CAC, other stromal pathologies adjacent and just underneath superficial lesions that induce shadowing may be obscured. However, improvements in ASOCT hardware with improved penetration while combined with advancements in post-processing techniques such as CAC may provide the best ASOCT image quality for such situations. Further study is required to investigate the potential clinical impact of the CAC, as this current early study was of a cross-sectional nature and used mainly to illustrate the potential use of CAC in ASOCT imaging, which may be established using future prospective clinical studies.

In conclusion, we have illustrated that applying CAC to the Spectralis ASOCT images provided the best overall image quality, but when CAC was not employed, the RTVue outperformed the other two devices. Overall, CAC was able to enhance corneal images by eliminating shadows, by making corneal layer boundaries more detectable, and by enhancing the visibility of the cornea against the image background. While the proposed image enhancements achieved by CAC are device-dependent and layer-specific, they may find wide applicability in corneal clinics.

Acknowledgments

Supported by grants from the Ministry of Education, Academic Research Funds, Tier 1 (R-397-000-181-112; R-397-000-140-133; MJAG) and from an NUS Young Investigator Award (NUSYIA_FY13_P03, R-397-000-174-133; MJAG), the donors of the NGR, a program of the BrightFocus Foundation (formerly American Health Assistance Foundation or AHAF), from the UK Department of Health through the award made by the UK National Institute for Health Research to Moorfields Eye Hospital NHS Foundation Trust and UCL Institute of Ophthalmology for a Biomedical Research Centre for Ophthalmology (NGS).

Disclosure: **C.W. Chung,** None; **M. Ang,** None; **M. Farook,** None; **N.G. Strouthidis,** None; **J.S. Mehta,** None; **J.M. Mari,** None; **M.J.A. Girard,** None

References

1. Whitcher JP, Srinivasan M, Upadhyay MP. Corneal blindness: a global perspective. *Bull World Health Organ*. 2001;79:214–221.
2. Foster A, Resnikoff S. The impact of Vision 2020 on global blindness. *Eye*. 2005;19:1133–1135.
3. Lim LS, Aung HT, Aung T, Tan DT. Corneal imaging with anterior segment optical coherence tomography for lamellar keratoplasty procedures. *Am J Opthalmol*. 2008;145:81–90.
4. Reim M, Kottek A, Schrage N. The cornea surface and wound healing. *Prog Retin Eye Res*. 1997;16:183–225.
5. Dayhaw-Barker P. Corneal wound healing: II. The process. *Int Contact Lens Clin*. 1995;22:110–116.
6. Dupps WJ Jr, Wilson SE. Biomechanics and wound healing in the cornea. *Exp Eye Res*. 2006; 83:709–720.
7. Wirbelauer C, Scholz C, Haberle H, Laqua H, Pham DT. Corneal optical coherence tomography before and after phototherapeutic keratectomy for recurrent epithelial erosions(2). *J Cataract Refract Surg*. 2002;28:1629–1635.
8. Tan DT, Dart JK, Holland EJ, Kinoshita S. Corneal transplantation. *Lancet*. 2012;379:1749–1761.
9. Wirbelauer C, Winkler J, Bastian GO, Haberle H, Pham DT. Histopathological correlation of corneal diseases with optical coherence tomography. *Graefes Arch Clin Exp Ophthalmol*. 2002;240:727–734.
10. Izatt JA, Hee MR, Swanson EA, et al. Micrometer-scale resolution imaging of the anterior eye in vivo with optical coherence tomography. *Arch Ophthalmol*. 1994;112:1584–1589.
11. Ang M, Chong W, Tay WT, et al. Anterior segment optical coherence tomography study of the cornea and anterior segment in adult ethnic South Asian Indian eyes. *Invest Ophthalmol Vis Sci*. 2012;53:120–125.
12. Ang M, Chong W, Huang H, et al. Comparison of anterior segment optical tomography parameters measured using a semi-automatic software to standard clinical instruments. *PloS One*. 2013; 8:e65559.

13. Samy El Gendy NM, Li Y, Zhang X, Huang D. Repeatability of pachymetric mapping using Fourier domain optical coherence tomography in corneas with opacities. *Cornea*. 2012;31:418–423.
14. Cavanagh HD, Petroll WM, Alizadeh H, He YG, McCulley JP, Jester JV. Clinical and diagnostic use of in vivo confocal microscopy in patients with corneal disease. *Ophthalmology*. 1993;100:1444–1454.
15. Pavlin CJ, Sherar MD, Foster FS. Subsurface ultrasound microscopic imaging of the intact eye. *Ophthalmology*. 1990;97:244–250.
16. Bianciotto C, Shields CL, Guzman JM, et al. Assessment of anterior segment tumors with ultrasound biomicroscopy versus anterior segment optical coherence tomography in 200 cases. *Ophthalmology*. 2011;118:1297–1302.
17. Hirano K, Ito Y, Suzuki T, Kojima T, Kachi S, Miyake Y. Optical coherence tomography for the noninvasive evaluation of the cornea. *Cornea*. 2001;20:281–289.
18. Khurana RN, Li Y, Tang M, Lai MM, Huang D. High-speed optical coherence tomography of corneal opacities. *Ophthalmology*. 2007;114:1278–1285.
19. Wirbelauer C, Scholz C, Hoerauf H, Engelhardt R, Birngruber R, Laqua H. Corneal optical coherence tomography before and immediately after excimer laser photorefractive keratectomy. *Am J Opthalmol*. 2000;130:693–699.
20. Wirbelauer C, Pham DT. Imaging and quantification of calcified corneal lesions with optical coherence tomography. *Cornea*. 2004;23:439–442.
21. Zhou SY, Wang CX, Cai XY, Huang D, Liu YZ. Optical coherence tomography and ultrasound biomicroscopy imaging of opaque corneas. *Cornea*. 2013;32:e25–e30.
22. Girard MJ, Ang M, Chung CW, et al. Enhancement of corneal visibility in optical coherence tomography images using corneal adaptive compensation. *Transl Vis Sci Technol*. 2015;4 (3):3.
23. Girard MJ, Strouthidis NG, Ethier CR, Mari JM. Shadow removal and contrast enhancement in optical coherence tomography images of the human optic nerve head. *Invest Ophthalmol Vis Sci*. 2011;52:7738–7748.
24. Mari JM, Strouthidis NG, Park SC, Girard MJ. Enhancement of lamina cribrosa visibility in optical coherence tomography images using adaptive compensation. *Invest Ophthalmol Vis Sci*. 2013;54:2238–2247.
25. Foin N, Mari JM, Nijjer S, et al. Intracoronary imaging using attenuation-compensated optical coherence tomography allows better visualisation of coronary artery diseases. *Cardiovasc Revasc Med*. 2013;14:139–143.
26. Foin N, Mari JM, Davies JE, Di Mario C, Girard MJ. Imaging of coronary artery plaques using contrast-enhanced optical coherence tomography. *Eur Heart J Cardiovasc Imaging*. 2013;14:85.
27. Girard MJ, Tun TA, Husain R, et al. Lamina cribrosa visibility using optical coherence tomography: comparison of devices and effects of image enhancement techniques. *Invest Ophthalmol Vis Sci*. 2015;56:865–874.
28. Li Y, Shekhar R, Huang D. Corneal pachymetry mapping with high-speed optical coherence tomography. *Ophthalmology*. 2006;113:792–799, e792.
29. Tan DT, Anshu A, Mehta JS. Paradigm shifts in corneal transplantation. *Ann Acad Med Singapore*. 2009;38:332–338.
30. Ang M, Cai Y, Shahipasand S, et al. En face optical coherence tomography angiography for corneal neovascularisation. *Br J Ophthalmol*. 2016;100:616–621.
31. Ang M, Sim DA, Keane PA, et al. Optical coherence tomography angiography for anterior segment vasculature imaging. *Ophthalmology*. 2015;122:1740–1747.
32. De Benito-Llopis L, Mehta JS, Angunawela RI, Ang M, Tan DT. Intraoperative anterior segment optical coherence tomography: a novel assessment tool during deep anterior lamellar keratoplasty. *Am J Opthalmol*. 2014;157:334–341, e333.
33. Wang Z, Bovik AC, Sheikh HR, Simoncelli EP. Image quality assessment: from error visibility to structural similarity. *IEEE Trans Image Process*. 2004;13:600–612.
34. van Velthoven ME, van der Linden MH, de Smet MD, Faber DJ, Verbraak FD. Influence of cataract on optical coherence tomography image quality and retinal thickness. *Br J Ophthalmol*. 2006;90:1259–1262.
35. Schmitt JM. Optical coherence tomography (OCT): a review. *IEEE J Sel Top Quantum Electron*. 1999;5:1205–1215.